Sequential Actions of Phospholipase D and Phosphatidic Acid Phosphohydrolase 2b Generate Diglyceride in Mammalian Cells

Vicki A. Sciorra and Andrew J. Morris*

Department of Pharmacological Sciences and Institute for Cell and Developmental Biology, State University of New York, Stony Brook, New York 11794-8651

Phosphatidylcholine (PC) is a major source of lipid-derived second messenger molecules that function as both intracellular and extracellular signals. PC-specific phospholipase D (PLD) and phosphatidic acid phosphohydrolase (PAP) are two pivotal enzymes in this signaling system, and they act in series to generate the biologically active lipids phosphatidic acid (PA) and diglyceride. The identity of the PAP enzyme involved in PLD-mediated signal transduction is unclear. We provide the first evidence for a functional role of a type 2 PAP, PAP2b, in the metabolism of PLD-generated PA. Our data indicate that PAP2b localizes to regions of the cell in which PC hydrolysis by PLD is taking place. Using a newly developed PAP2b-specific antibody, we have characterized the expression, posttranslational modification, and localization of endogenous PAP2b. Glycosylation and localization of PAP2b appear to be cell type and tissue specific. Biochemical fractionation and immunoprecipitation analyses revealed that PAP2b and PLD2 activities are present in caveolin-1–enriched detergent-resistant membrane microdomains. We found that PLD2 and PAP2b act sequentially to generate diglyceride within this specialized membrane compartment. The unique lipid composition of these membranes may provide a selective environment for the regulation and actions of enzymes involved in signaling through PC hydrolysis.

INTRODUCTION

Products of lipid metabolism serve a critical role as second messengers in various cellular signaling pathways (Divecha and Irvine, 1995). The best-characterized signaling pathway is the production of two second messengers, diglyceride (DG) and *myo*-inositol 1,4,5 trisphosphate (IP_3) generated by phosphoinositide-specific phospholipase C-catalyzed hydrolysis of phosphatidylinositol 4,5 bisphosphate ($PI(4,5)P_2$). IP_3 mobilizes calcium by binding to intracellular receptors (Berridge, 1993), whereas diacylglycerol binds and activates members of the conventional and novel classes of protein kinase C (PKC) isoenzymes (Nishizuka, 1995). It was be-

lieved that this pathway is the primary mechanism for generation of DG in stimulated cells; however, it is now evident that phosphatidylcholine (PC) and not $PI(4,5)P_2$ is a significant source of DG in many agonist-stimulated cells (Exton, 1997).

The generation of DG from PC has been attributed to the direct action of a putative PC–phospholipase C or to the sequential actions of phospholipase D (PLD) and phosphatidic acid phosphohydrolase (PAP) (Singer *et al.*, 1997). Recently, much attention has been focused on the role of PC-specific PLD in cell signaling (Exton, 1997). PLD catalyzes the hydrolysis of PC to yield phosphatidic acid (PA) and choline. Molecular characterization indicates that there are at least two distinct isoforms of PLD in mammalian cells (Hammond *et al.*, 1995; Colley *et al.*, 1997). Phosphatidic acid (PA) is a biologically active lipid implicated in many cellular processes, including cytoskeletal reorganization, regulated secretion, and the respiratory burst in neutrophils (Exton, 1997). PA has also been found to interact with the proto-oncogenic Raf-1 kinase (Ghosh *et al.*, 1996) and to be critical for Raf-1 translocation in stimulated cells (Ghosh *et al.*, 1996; Rizzo *et al.*, 1999).

In addition to its putative roles in cell signaling, PA can be rapidly metabolized to several other second messenger mol-

* Corresponding author. E-mail address: andrew@pharm.sunysb.edu.
  Abbreviations used: β-DOG, octyl-β-D-glucopyranoside; BODIPY-PC, 2-decanoyl-1-{O-[11-(4,4-difluoro-5, 7-dimethyl-4-bora-3a, 4a-diazasindacene-3-propionyl) amino] undecyl}-*sn*-glycero-3-phosphocholine; DG, diglyceride; DRMs, detergent-resistant membrane domains; Endo H, endoglycosidase H; HEK, human embryonic kidney; PA, phosphatidic acid; PAP, phosphatidic acid phosphohydrolase; PLD, phospholipase D; PKC, protein kinase C; PMA, phorbol 12-myristate 13-acetate; $PI(4,5)P_2$, phosphatidylinositol 4,5 bisphosphate.

ecules. PA can be hydrolyzed by phospholipase A_2 (PLA_2) to form *lyso*PA, which is a potent mitogen, acting through G protein–coupled cell surface receptors. PAP-catalyzed dephosphorylation of PA generates DG, which can serve as a direct precursor to triglycerides and membrane phosphoglycerolipids (Smith *et al.*, 1957) or act as a second messenger (Nishizuka, 1995). Degradation of PC by the PLD/PAP pathway is now considered to be an important route of DG formation in stimulated cells (Exton, 1997). PAP could therefore play a critical role in maintaining the balance between signaling molecules PA and DG and in the salvage of both of these agonist-sensitive molecules for general glycerolipid synthesis (Brindley and Waggoner, 1996).

Jamal *et al.* (1991) first identified two types of mammalian PAP enzymes based on subcellular localization and biochemical properties in rat liver. Type 1 PAP (PAP1) activity is present in the cytosol and endoplasmic reticulum (ER). Its catalytic activity is Mg^{2+}-dependent and sensitive to sulfhydryl-reactive reagents such as *N*-ethylmaleimide. PAP1 translocates from a cytosolic to particulate fraction on stimulation of hepatocytes with glucagon and as such is thought to be involved in glycerolipid biosynthesis (Brindley and Waggoner, 1996); however, PAP1 has not been purified from any mammalian source and thus little is known about its molecular structure and function. On the other hand, the type 2 PAP (PAP2) has been purified from membranes of porcine thymus (Kanoh *et al.*, 1992) and rat liver (Waggoner *et al.*, 1995). Unlike PAP1, PAP2 activity is independent of Mg^{2+} and insensitive to *N*-ethylmaleimide. Recently, Kai *et al.* (1997) reported the cloning of two human isoforms of PAP2 that are designated PAP2a and PAP2b. A third isoform, PAP2c, has since been identified (Hooks *et al.*, 1998; Roberts *et al.*, 1998). Sequence analysis and biochemical data indicate that these PAPs are small integral membrane glycoproteins. PAP2a appears to be homologous to the mouse 35-kDa PAP2, a glycoprotein found in the plasma membrane (Kai *et al.*, 1996). PAP2b is the human homologue of a previously characterized rat protein named Dri42. The rat Dri42 protein is an ER resident protein that is up-regulated during epithelial differentiation (Barila *et al.*, 1996). PAP2 enzymes can also hydrolyze other lipid phosphates in vitro, such as ceramide-1-phosphate, sphingosine-1-phosphate, and lysoPA, in addition to PA (Waggoner *et al.*, 1996; Kai *et al.*, 1997; Roberts *et al.*, 1998). This suggests that PAP2 enzymes may also participate in the regulation of several lipid signaling systems. It is not clear which of these lipid phosphates are physiological substrates for the PAP2 enzymes.

Here, we present evidence for a functional role for PAP2b in the metabolism of PA derived from PLD activation. We report that the PLD/PAP pathway is operational in detergent-resistant membrane microdomains (DRMs), a type of specialized membrane compartment implicated in vesicular trafficking and signal transduction (Brown and London, 1998). PLD activity (most likely PLD2) and PAP2b localize to and act sequentially to generate DG in these specialized domains. We propose that the functional association between PLD and PAP2b is accomplished by colocalization of these enzymes to the same membrane compartments and discuss the potential significance of these findings related to their regulation and function in cell signaling.

MATERIALS AND METHODS

Materials

Tunicamycin, protein-*N*-glycanase F, and Endo H were from Boehringer Mannheim (Indianapolis, IN). Mouse monoclonal anticaveolin-1, rabbit polyclonal anticaveolin-1, mouse monoclonal anti-Rab5, and mouse monoclonal anticalnexin were purchased from Transduction Labs (Lexington, KY). Rabbit polyclonal anticalnexin (StressGen Biotech, Victoria, British Columbia, Canada) and mouse monoclonal mouse anti-BiP (StressGen) were kind gifts from Jim Trimmer (State University of New York [SUNY] at Stony Brook). Monoclonal mouse anti-transferrin receptor was purchased from Zymed (San Francisco, CA), and mouse monoclonal anti-α adaptin was purchased from Affinity Bioreagents (Golden, CO). Horseradish peroxidase-conjugated anti-mouse or anti-rabbit were from Amersham (Arlington Heights, IL). Rhodamine-conjugated goat anti-rabbit IgG and fluorescein-conjugated goat anti-mouse IgG were from Cappel (West Chester, PA). Affinity-purified PLD1 and PLD2 anti-peptide antibodies were from Quality Controlled Biochemicals (Hopkinton, MA), as previously described (Colley *et al.*, 1997; Hammond *et al.*, 1997). [^{32}P]-γ-ATP, Trans [^{35}S] Label, [^{32}P]-PO_4^2, and [9,10 ^{3}H(N)] palmitic acid were from ICN Biochemicals (Costa Mesa, CA). Lipids were purchased from Avanti Polar Lipids (Alabaster, AL) unless stated otherwise. DG kinase was purchased from Calbiochem (La Jolla, CA). All other reagents used were of the highest grade.

Cell Culture

Swiss 3T3 fibroblasts were obtained from American Type Culture Collection (CCL 92, received at passage 116). Human embryonic kidney (HEK) 293 cells, COS7 cells, and Sf9 cells were obtained from the Tissue-culture Core Facility at SUNY at Stony Brook. Cells were cultured in DMEM (Life Technologies, Gaithersburg, MD) supplemented with 10% fetal calf serum (Gemini, Calabasas, CA), 100 U/ml penicillin–streptomycin, and 0.22% $NaHCO_3$. Swiss 3T3 cells were maintained in 75-cm^2 flasks and subcultured at 3- to 4-d intervals. For the experiments described herein, Swiss 3T3 cells were used between passages 118 and 130. Sf9 cells were maintained at 27°C in complete Grace's medium (Life Technologies) supplemented with lactalbumin, yeastolate, and 10% fetal bovine serum containing antibiotic–antimycotic reagents. Monolayers of exponentially growing Sf9 cells cultured in completed Grace's medium (generally 2×10^7 cells/225-cm^2 flask) were infected with recombinant baculoviruses for expression of the PAP2 or PLD enzymes at a multiplicity of 10. The cells were cultured for 48 h at 27°C. Extracts were prepared as previously described (Roberts *et al.*, 1998).

Preparation of Affinity-purified PAP Anti-Peptide Antibodies

A peptide corresponding to residues 2–17 (QNYKYDKAIVPESKNG) of the sequence of human PAP2b was synthesized. Rabbits were immunized, and antibody titers were determined by enzyme-linked immunosorbent assay using the individual peptide antigen as the solid phase. Antibodies were purified by affinity chromatography using the individual immobilized peptide antigen as described (Harlow and Lane, 1988). Selectivity of the antibodies was determined by detection of recombinantly expressed PAP enzymes by Western blotting. Quality Controlled Biochemicals prepared the peptide antisera.

Mammalian Cell Expression Constructs and Cell Transfections

The PAP2a and PAP2b cDNAs were subcloned into the *Eco*RI and *Xba*I sites of pcDNA (Invitrogen, San Diego, CA). HEK 293 cells were plated into six-well dishes that had been precoated with poly-L-lysine hydrobromide (Sigma, St. Louis, MO) and grown to

50–60% confluence. Transfections were performed using Lipofectamine and OPTI-MEM medium (Life Technologies) and 1–5 μg of DNA per well. Control cells were transfected with the appropriate empty vector DNAs to keep amounts of transfected DNA constant. The DNA-containing medium was removed from the plate (overnight incubation) and replaced by DMEM containing 10% FBS. Experiments were performed 24 h after transfection.

Isolation of DRMs

DRMs were isolated as described previously by Brown and Rose (1992), with slight modifications. Swiss 3T3 cells were grown to confluence at 37°C in 100-mm culture dishes (4 d with one change of DMEM). Cells were washed twice in ice-cold PBS (80 mM disodium hydrogen orthophosphate, 20 mM sodium dihydrogen orthophosphate, 100 mM sodium chloride) and lysed in 1 ml of buffer A (25 mM HEPES, pH 7.4, 150 mM NaCl, 5 mM EDTA, 5 mM EGTA, 10 mM sodium pyrophosphate, 40 mM β-glycerophosphate, 50 mM sodium fluoride, 1 mM DTT, 0.1 mM PMSF, 0.5 mM sodium orthovanadate, 0.1 mM benzamidine, 10 μg/ml leupeptin, and 10 μg/ml aprotinin) containing 1% Triton X-100 (TX100; Bio-Rad, Hercules, CA) on ice for 30 min. Cells were scraped (two dishes per gradient), and 2.5 ml of buffer A containing 80% sucrose was added, mixed, and transferred to an SW41 ultracentrifuge tube (Beckman, Fullerton, CA). A linear sucrose gradient (5–38% in buffer A) was layered over the lysate. Gradients were centrifuged for 16–18 h at 28-K rpm at 4°C in a Beckman SW41 rotor. Fractions (1 ml) were collected from the top of the gradient. When indicated, DRMs (at the 5–38% interface) were collected with a syringe, washed in PBS, and pelleted by centrifugation at 28-K rpm for 1 h at 4°C.

Subcellular Fractionation

Postnuclear supernatants were prepared by resuspending cell pellets in TSE (50 mM Tris, pH 7.4, 250 mM sucrose, and 1 mM EDTA) containing protease inhibitors and sonicated (three 5-s bursts set on 10% output of a VirSonic probe sonicator, Virtis Instruments, Gardinier, NY) on ice. Lysates were centrifuged at $1000 \times g$ for 5 min at 4°C. Postnuclear supernatants were further centrifuged for 1 h at $100,000 \times g$ at 4°C to obtain a cytosolic fraction. The remaining pellet was resuspended in TSE buffer (equal volume as above) containing 1% TX100 and incubated for 1 h at 4°C with gentle agitation, followed by centrifugation at $100,000 \times g$ at 4°C for 1 additional hour. The insoluble pellet was resuspended in TSE buffer (equal volume as above) containing 1% octyl-β-D-glucopyranoside (β-DOG) and centrifuged for 5 min at $1000 \times g$. For PLD analysis, total membranes were resuspended in TSE buffer without TX100 and probe-sonicated extensively on ice.

Immunoprecipitation

Confluent cells grown in 100-mm dishes were washed with ice-cold PBS and scraped in PBS containing 0.1 mM PMSF, 0.1 mM benzamidine, 10 μg/ml leupeptin, and 0.5 mM sodium orthovanadate. Cells were pelleted by gentle centrifugation and resuspended in buffer A + 1% TX100 + 1% β-DOG (Jersey Lab Supply, Rahway, NJ). Cells were incubated at 4°C for 30 min with gentle agitation. Lysates were centrifuged at $1000 \times g$ for 5 min at 4°C. Supernatants were centrifuged again at $15,000 \times g$ for 20 min at 4°C. PAP2b was immunoprecipitated directly from this fraction. Aliquots (1 ml) (200–400 μg of protein diluted with PBS) were incubated with 3–5 μg of affinity-purified antibody for 2 h at 4°C. Protein A-Sepharose (Sigma) was then added (40 μl of a 1:1 mixture of protein A/PBS), followed by a further incubation for 2 h at 4°C. Immune complexes were sedimented by gravitation on ice for 30 min, washed three times with 1 ml of buffer A + 1% TX100, and washed four times with 1 ml of PBS. DRMs were resuspended in buffer A + 1% TX100 and warmed at 37°C for 5 min. Aliquots were diluted with PBS and immunoprecipitated as described above. Immune complexes were

boiled in sample buffer for Western blot analysis. For endogenous PLD immunoprecipitation analysis, membrane sonicates (see Subcellular Fractionation) were incubated with 1% NP40 for 1 h at 4°C before immunoprecipitation (Rudge *et al.,* 1998a).

Western Blot Analysis

Protein concentration was determined by the method of Bradford (1976) using BSA as a standard. Samples were prepared for SDS-PAGE by boiling in sample buffer. Proteins were electrophoretically transferred onto nitrocellulose membranes (Bio-Rad) for 2 h at 200 mA at 4°C. Blots were blocked in 5% nonfat dry milk in TBS with 0.1% Tween-20 (vol/vol) (TBST) for 2 h at room temperature. Primary antibody incubations were performed in PBS containing 4% BSA for 2 h at room temperature or overnight at 4°C. Secondary antibody incubations were performed in TBST containing 5% nonfat dry milk at 1:10,000 for 1 h at room temperature. Protein bands were visualized by enhanced chemiluminescence using Super Signal (Pierce, Rockford, IL). Films were scanned with a Bio-Rad (Hercules, CA) scanning densitometer.

Indirect Immunofluorescence

Swiss 3T3 cells or COS7 cells were grown directly on sterilized glass coverslips. HEK 293 cells were grown on poly-L-lysine–coated glass coverslips, and transfected with pcDNA–hPAP2b before processing. Cells were washed three times with ice-cold PBS containing 1 mM MgCl$_2$ and 1 mM CaCl$_2$, fixed by incubation in 4% paraformaldehyde (in PBS) for 20 min at 4°C, and permeabilized with PBS containing 0.1% TX100 (Pierce) for 10 min at 4°C. Fixed cells were incubated for 30 min with blocking buffer (4% nonfat dry milk in TBS + TX100) followed by a 1-h incubation with rabbit polyclonal antibody against PAP2b (1:100) in blocking buffer (or overnight at 4°C). Coverslips were washed followed by a 30-min incubation with rhodamine-conjugated goat anti-rabbit IgG (1:200). Coverslips were rinsed extensively and mounted in antifade reagent (VectaShield, Burlingame, CA). For double-labeling experiments, fixed cells were incubated with rabbit anti-PAP2b at 1:200 and mouse anti-BiP (1:200) for 1 h, washed, and stained with rhodamine-conjugated goat anti-rabbit IgG and fluorescein-conjugated goat anti-mouse IgG. For Golgi labeling, Swiss 3T3 cells were incubated with 2 μM (1-caproyl-2-[6-[(7-nitro-2–1,3-benzoxadiazol-4-yl)amino]caproyl]-2n-glycerol-3) NBD-ceramide (Molecular Probes, Eugene, OR) in serum-free media for 10 min at 37°C. The medium was then removed, and cells were further incubated in serum-free medium containing 0.68 mg/ml fatty acid-free BSA for 30 min. NBD-ceramide–labeled cells were fixed (omitting TX100) and mounted as described above. Stained cells were viewed by confocal laser scanning epifluorescence microscopy using a Nikon Diaphot microscope equipped with a 40× (NA 1.4) PlanApo objective oil immersion lens. Epifluorescent images were captured with an Optronics color camera and processed using Image I software and Adobe Photoshop 3.0. Control images were acquired and processed in exactly the same way as their corresponding image.

DG Measurements

Cellular lipids were extracted by the method of Bligh and Dyer (1959), and DG mass was determined as described in Cook and Wakelam (1992). Briefly, lipid extracts were resuspended in 50 μl of 0.6% TX100 containing phosphatidylserine. Reactions contained [^{32}P]-γ-ATP (2–10 μCi/50 nmol) and 0.1 U of DG kinase (Calbiochem) and were incubated for 1 h at 37°C. Lipids were extracted and analyzed by thin-layer chromatography (TLC). PA was identified by autoradiography, scraped from the plate, and radioactivity was quantitated by liquid scintillation counting. DG mass was calculated by extrapolation from a known DG mass standard curve. In some cases, a fraction of the lipid extract was removed for determination of total lipid phosphorous after wet digestion in perchloric acid (Morris *et al.,* 1995).

Table 1. PAP2b couples with endogenous PLD in HEK 293 cells to generate diglyceride

	DG (pmol/nmol Pi)[a]						PAP2 in vitro activity[b]	PLD in vivo activity[c]
	− PMA			+ PMA				
	Control	2-BuOH	1-BuOH	Control	2-BuOH	1-BuOH		
Vector	17 ± 1	16 ± 1	16 ± 2	42 ± 3	37 ± 4	25 ± 5	22 ± 1	2.2 ± .4
PAP2a	23 ± 2	20 ± 8	24 ± 2	47 ± 5	36 ± 4	26 ± 4	366 ± 6	2.1 ± .4
PAP2b	32 ± 2	29 ± 4	26 ± 3	87 ± 10	79 ± 5	54 ± 8	265 ± 11	2.2 ± .2

[a] DG amounts were determined using DG kinase (Calbiochem) and ^{32}P γ-ATP, normalized to lipid phosphate, and expressed as the means ± SD of triplicate determinations from two experiments.

[b] Equal amounts of cell sonicates were assayed for PAP2 activity using 100 μM PA without Mg^{+2}. Activity is expressed as picomoles per 30 min per milligram.

[c] PLD activity was measured as the fold increase in [^{3}H]-phosphatidylbutanol in PMA-stimulated cells over unstimulated cells. Results are the means ± range from two experiments.

PAP and PLD Activity Measurements

[^{32}P]-PA was prepared by phosphorylation of 1,2-dioleoyl-sn-glycerol using *Escherichia coli* DG kinase and γ[^{32}P]-ATP as described in Cook and Wakelam (1992). PAP activity assays were performed using [^{32}P]-PA (Roberts *et al.*, 1998) or NBD-phosphatidic acid (NBD-PA; Avanti Polar Lipids, Alabaster, AL) as substrate (1:10, PA/TX100). Immune complexes containing PLD were suspended in PBS and assayed in PLD assay buffer (Brown *et al.*, 1993). Lipid vesicles containing 3 μM 2-decanoyl-1-{O-[11-(4,4-difluoro-5, 7-dimethyl-4-bora-3a, 4a-diazasindacene-3-propionyl) amino] unde-cyl}-sn-glycero-3-phospho-choline (BODIPY-PC; Molecular Probes), 92 μM phosphatidylethanolamine, and 5 μM PI(4,5)P$_2$ (purified as described in Morris *et al.*, 1995) were prepared by bath sonication of dry lipid films. Reactions were initiated by warming at 37°C for 30 min and terminated by the addition of 200 μl of methanol containing 2% acetic acid. Lipids were extracted by the method of Bligh and Dyer (1959) and separated by TLC as described (Rudge *et al.*, 1998a, b). Fluorescence of lipid products was quantitated using a plate-reading fluorometer at 485 nm excitation and 530 nm emission as described (Rudge *et al.*, 1998a,b). ADP-ribosylation factor (Arf-1), RhoA, and PKCα were prepared as described (Hammond *et al.*, 1997), and concentrations of each protein that gave maximal activation of recombinant human PLD1 were used in the subsequent studies.

RESULTS

### PAP2b Couples to an Endogenous PLD in HEK 293 Cells

In the presence of a primary but not secondary alcohol (i.e., 1-butanol vs. 2-butanol), PLD catalyzes a unique transphosphatidylation reaction generating a phosphatidylalcohol at the expense of PA (Pai *et al.*, 1988). Rumenapp *et al.* (1997) reported that phorbol 12-myristate 13-acetate (PMA) stimulates a PLD activity in HEK 293 cells. Consistent with these observations, stimulation of vector-transfected HEK 293 cells (control) with a maximally effective concentration of PMA (100 nM) for 30 min increased phosphatidylbutanol levels approximately twofold (Table 1). Phosphatidylalcohols are not substrates for PAP (Metz and Dunlop, 1991), and consequently the generation of DG via the PLD/PAP pathway will be reduced. We found that the PMA-dependent increases in DG levels were significantly attenuated by pretreatment of the cells with 30 mM 1-butanol but not with 30 mM 2-butanol (Table 1). These data demonstrate that HEK 293 cells express a PAP activity that can couple to a PKC-responsive PLD.

To investigate the role of the newly identified type 2 PAP isoenzymes in PLD-dependent DG formation, PAP2a and PAP2b were expressed in HEK 293 cells by transient transfection, and DG levels were measured under conditions known to provoke PLD-catalyzed PC hydrolysis (i.e., PMA treatment). In vitro PAP assays verified that PAP2a and PAP2b were expressed as active proteins in HEK 293 cells (16- and 12-fold, respectively [Table 1]). Despite the dramatic increase in PAP activity observed in vitro, DG levels in cells after serum starvation were only increased 1.4- and 1.9-fold by the overexpression of PAP2a and PAP2b, respectively (Table 1). Although we consistently saw no effect of 2-butanol on basal levels of DG in PAP2b-expressing cells (Table 1), the effect of 1-butanol on basal levels of DG was more variable. Occasionally, 1-butanol was found to reduce the basal levels of DG in PAP2b-expressing cells (our unpublished results), suggesting the involvement of a PLD. Alternatively, increased DG levels (butanol insensitive) observed in PAP2a- and PAP2b-expressing cells may be a consequence of a reduction of steady-state levels of PA (de novo). Reduction in steady-state levels of PA by the overexpression of PAP2a has been reported in ECV304 endothelial cells (Leung *et al.*, 1998).

Stimulation of vector-transfected cells with PMA produced a 2.5-fold increase in DG levels. Surprisingly, expression of PAP2b (5.1-fold; Table 1), and not PAP2a (2.8-fold; Table 1), in these cells resulted in a significantly enhanced level of DG when stimulated with PMA as compared with the levels in unstimulated vector-transfected cells. In parallel experiments, PMA-stimulated PLD activity (in the presence of 1-butanol) was measured by the formation of phosphatidylbutanol in HEK 293 cells expressing PAP2a or PAP2b using endogenously labeled phospholipid substrates. Expression of either PAP2a or PAP2b did not elevate intrinsic PLD activity compared with the vector-transfected control (Table 1). Therefore, the elevation in DG seen in PAP2b-expressing PMA-stimulated cells is not a consequence of an increased level of PLD activity. Collectively, these results

Figure 1. Specificity and efficiency of the PAP2b antibody. (A) Sequence alignment of the N-terminal region of hPAP2a, hPAP2b, hPAP2c, and mouse PAP2b (expressed sequence tag AU03 6086). A peptide corresponding to residues 2–17 of the sequence of human PAP2b (letters in bold) was prepared and used to immunize rabbits as described in MATERIALS AND METHODS. (B) Fifty micrograms of total protein from TX100/βDOG lysates of baculovirus-infected Sf9 cells expressing hPAP2a, hPAP2b, or hPAP2c were subjected to immunoprecipitation using the anti-peptide PAP2b antibody. Ten micrograms of protein from lysates and one-twentieth of each immunoprecipitate (IP) were separated (12.5% SDS-PAGE), transferred, and analyzed for PAP2b by Western blotting. (C) PAP2 activity in the IP was determined and expressed as the percentage activity in the IP of the total PAP2 activity in the corresponding lysate

(mean ± SD of triplicate determinations). (D) One hundred micrograms of protein from TX100/β-DOG lysates of baculovirus-infected Sf9 cells expressing hPAP2b were heated at 80°C for 3 min, then cooled on ice for an additional 5 min. Lysates were incubated in the presence or absence of PNGase F (1 U per assay) for 12 h at 37°C. Samples were boiled in sample buffer for 5 min to quench the reaction. Twenty micrograms of protein per lane were separated by SDS-PAGE (12.5%) and transferred to nitrocellulose membranes. Membranes were probed with PAP2b antibody or PAP2b antibody that was preabsorbed with 200-fold excess of the corresponding peptide.
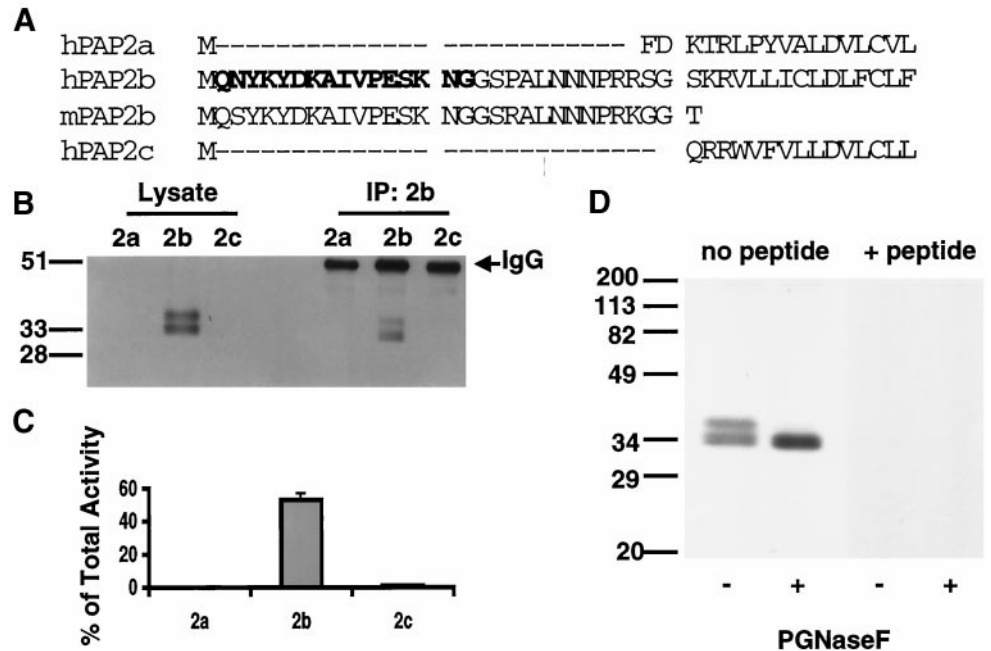
demonstrate that expression of PAP2b in HEK 293 cells produces an enzyme that has the capability to act sequentially with endogenous PLD to generate DG. We therefore focused our studies on PAP2b.

Generation and Characterization of an Anti-Peptide PAP2b Antibody

To characterize native PAP2b, a polyclonal antibody was generated against a peptide corresponding to N-terminal amino acid residues 2–17 of the deduced human PAP2b sequence (Figure 1A) as described in MATERIALS AND METHODS. This sequence of amino acid residues is present in Dri42, the rat homologue of human PAP2b (Barila *et al.*, 1996), and mouse PAP2b but absent from PAP2a, PAP2c, and a fourth mammalian PAP2 homologue, PAP2d (our unpublished results) (Figure 1A). Consequently, the antibody was expected to specifically recognize PAP2b from different species. The affinity-purified antibody against PAP2b detected a major species of 30–33 kDa in extracts of baculovirus-infected Sf9 cells expressing human PAP2b and a doublet of slightly slower mobility on SDS-PAGE (Figure 1B). This is in agreement with the predicted molecular weight (M_r ~35 kDa) as well as the molecular weight previously observed in HEK 293 cells transfected with PAP2b containing an epitope tag at the C terminus (Kai *et al.*, 1997).

The selectivity of this antibody was confirmed by immunoblotting and immunoprecipitation from lysates of baculovirus-infected Sf9 cells expressing human PAP2a, PAP2b, or PAP2c, which cause dramatic increases in membrane-associated PAP

activity as reported previously (Roberts *et al.*, 1998). As shown in Figure 1B, the PAP2b antibody was selective in detecting the recombinant PAP2b protein (Figure 1B) and immunoprecipitated PAP2 activity and protein only from cells expressing PAP2b (Figure 1, B and C). The specificity of the antibody was also examined by preabsorbing the antibody with competing peptide before Western analysis (Figure 1D). Inclusion of the peptide blocked the staining of all bands observed. In addition, the slower migrating forms were completely converted to the faster-migrating form when lysates were treated with peptide-*N*-glycosidase F (PNGase F), an enzyme that hydrolyzes most *N*-linked glycan chains from glycoproteins (Figure 1D). These results demonstrate that the other bands detected by the antibody most likely represent glycosylated forms of the enzyme, which has been described previously (Kai *et al.*, 1997).

Expression and Posttranslational Modification of Endogenous PAP2b

Most tissues are capable of dephosphorylating PA (Brindley and Waggoner, 1998) with specific activities being highest in rat brain, lung, kidney, and spleen (Waggoner *et al.*, 1995). Using our PAP2b antibody, protein expression in various tissues from an adult mouse was examined by Western blotting. As shown in Figure 2A, PAP2b was differentially expressed in the tissues examined with the highest level of expression in brain, then kidney and lung. In addition to a 30- to 33-kDa immunoreactive species, we detected immunoreactive species of slower mobility that were present in some (i.e., brain) but not all (i.e., liver) tissues examined. We found that PAP2b is highly
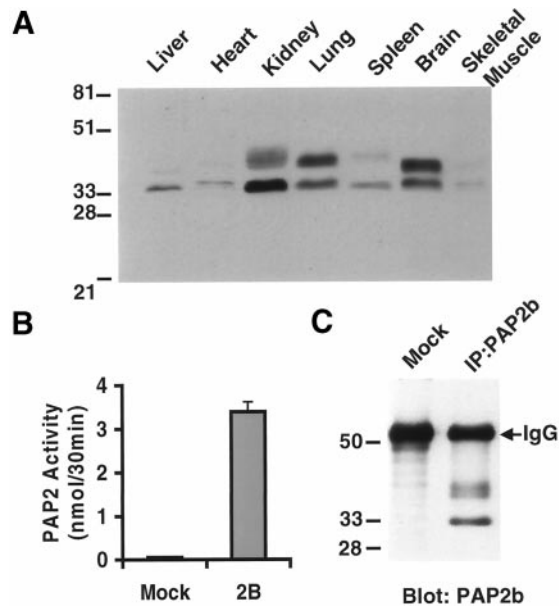
Figure 2. Expression of endogenous PAP2b. (A) Tissues from a female adult mouse were dissected, washed in PBS, and Dounce-homogenized 10–20 strokes in TSE buffer (50 mM Tris, pH 7.4, 250 mM sucrose, and 1 mM EDTA) on ice. Homogenates were centrifuged at $2000 \times g$ for 15 min to remove debris. One hundred micrograms of protein from the indicated tissue homogenate were separated (12.5% SDS-PAGE), transferred, and analyzed for PAP2b by Western blotting. (B) PAP2b was immunoprecipitated from 300 μg of protein from Swiss 3T3 cell detergent lysate and assayed for PAP activity using 100 μM PA/1 mM TX-100 per assay for 30 min at 37°C. "Mock" represents immunoprecipitation using an irrelevant IgG. (C) Each IP from B was separated (12.5% SDS-PAGE), transferred, and analyzed for PAP2b by Western blotting. Results are expressed as the means of triplicate immunoprecipitates (IP). Results are representative of three independent experiments.

expressed in Swiss 3T3 fibroblasts, and this cell line was used to characterize the endogenous enzyme. PAP2 activity (Figure 2B) and protein (Figure 2C) can be detected in immune complexes isolated by using the PAP2b antibody from Swiss 3T3 cell lysate. As observed in several mouse tissues, two immunoreactive species of PAP2b were detected of ~30–33 kDa and 35–40 kDa (Figure 2C), which were slightly different in molecular weight than the baculovirus-expressed recombinant counterpart. These differences observed in tissues and cells most likely represent heterogeneous populations of glycosylated species.

It has been previously shown that overexpressed, epitope-tagged PAP2b is glycosylated in mammalian cells (Barila *et al.*, 1996; Kai *et al.*, 1997). Because high expression and/or the introduction of a foreign epitope into a protein may alter its posttranslational processing, the modification and trafficking of endogenously expressed PAP2b was examined in Swiss 3T3 cells. Tunicamycin inhibits the biosynthesis of dolichol pyrophosphate *N*-acetyl-glucosamine and is often used to inhibit *N*-linked glycosylation in vivo. Swiss 3T3 cells grown in the presence of tunicamycin expressed only the faster-migrating species of PAP2b (Figure 3A). To confirm that PAP2b is modified with *N*-linked glycans, Swiss 3T3 cell lysates were incubated in the presence or absence of
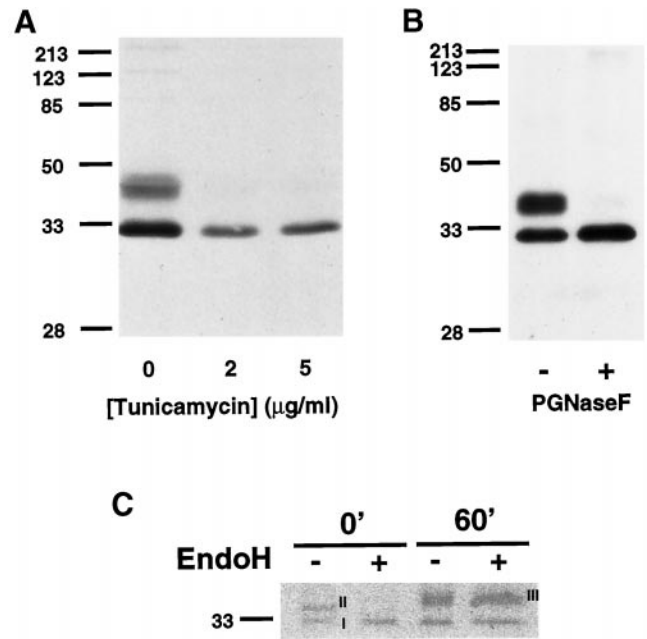

Figure 3. Posttranslational modification of endogenous PAP2b in Swiss 3T3 Cells. (A) Swiss 3T3 cells (80% confluence) were grown in the presence of tunicamycin for 18 h at 37°C. Postnuclear supernatants (60 μg/lane) were prepared and analyzed for PAP2b by Western blotting. (B) Lysates were incubated with PNGase F (1 U per assay) for 12 h at 37°C as described in legend to Figure 1. Forty micrograms of protein per lane were separated by SDS-PAGE (12.5%) and analyzed for PAP2b by Western blotting. (C) Swiss 3T3 cells were labeled with 300 μCi per 100-mm dish of Trans-^{35}S-Label (ICN) for 10 min, the media were removed, and cells were incubated in chase media containing 10 mM unlabeled methionine. PAP2b was immunoprecipitated, incubated with (+) or without (−) Endo H (10 mU per IP), and analyzed by SDS-PAGE (12.5%). A fluorogram of the gel is shown. Similar results were obtained in two additional experiments.

PNGase F. As shown in Figure 3B, the slower migrating species of PAP2b is reduced to the faster-migrating form of mobility similar to that observed with tunicamycin treatment. These data suggest that the faster-migrating species of PAP2b is a nonglycosylated form.

It is surprising that a considerable amount of PAP2b exists in a nonglycosylated state. To examine glycosylation in more detail, Swiss 3T3 cells were pulse-labeled with [^{35}S]-methionine, and endogenous PAP2b was immunoprecipitated and analyzed for susceptibility to Endo H at time 0 or after a 60-min chase with unlabeled methionine. *N*-linked glycans become resistant to Endo H digestion when modified in the medial cisternae of the Golgi (Brown and Rose, 1992, references therein). Two forms (I and II) are present before the chase but only form II is sensitive to Endo H (Figure 3C). This suggests that form II is "core glycosylated" in the ER or *cis*-Golgi but disappears after the chase. Form III appears in the 60-min chase and is resistant to Endo H. This most likely represents PAP2b with fully processed oligosaccharides acquired in the *trans*-Golgi network (Figure 3C). It is curious that a significant level of the presumably nonglycosylated form (I) still remains after the chase (Figure 3C).
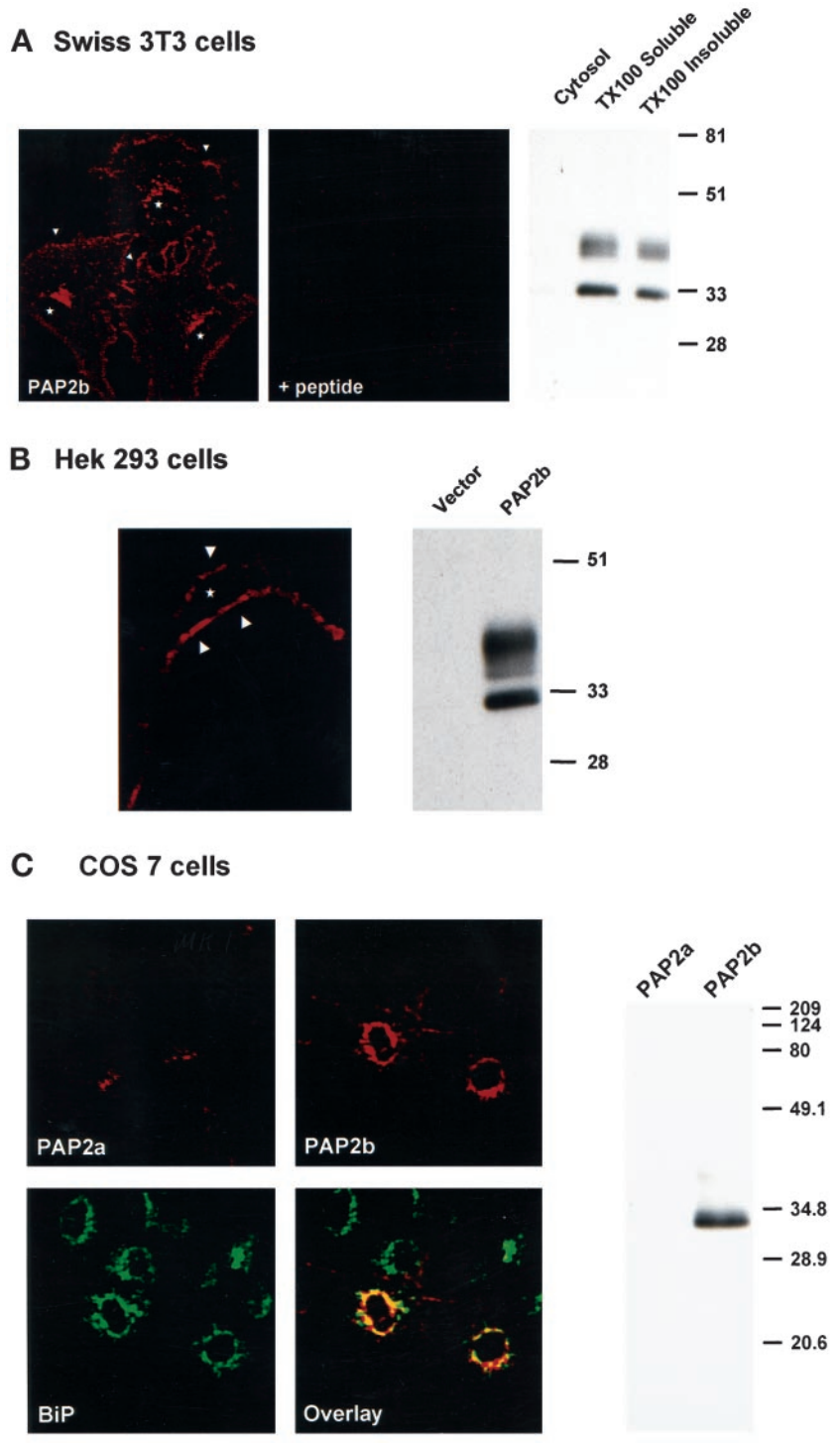
A Swiss 3T3 cells

B Hek 293 cells

Figure 4. Subcellular localization of PAP2b. (A, left) Swiss 3T3 cells were grown on coverslips and processed for confocal immunofluorescence localization using anti-PAP2b and rhodamine-conjugated goat anti-rabbit IgG (arrows indicate staining of cell periphery; stars indicate position of nuclei). Swiss 3T3 cells were also incubated with anti-PAP2b antibody that was preabsorbed with competing peptide before staining with secondary antibody (+peptide). (A, right) Swiss 3T3 cells were separated into cytosolic, TX100-soluble, and TX100-insoluble fractions (equal cell equivalents) and analyzed for PAP2b by Western blotting (12.5% SDS PAGE). (B, left) HEK 293 cells were grown on poly-L-lysine–coated coverslips and transfected with pcDNA-PAP2b using Lipofectamine as described in MATERIALS AND METHODS before processing. A representative confocal image (27 total; taken at 1 μM optical cross section [x–y]) is shown (arrows indicate cell periphery; star indicates position of nucleus). (B, right) HEK 293 cells transfected with pcDNA (Vector) or pcDNA-hPAP2b were analyzed for PAP2b by Western blotting (10 μg/lane). (C, left) COS7 cells were grown on coverslips and transiently transfected with pcDNA-PAP2a or pcDNA-PAP2b. Cells were labeled with rabbit anti-PAP2b and mouse anti-BiP antibodies. Cells were then stained with rhodamine-conjugated anti-rabbit IgG and fluorescein-conjugated anti-mouse IgG antibodies and examined by confocal fluorescence microscopy. The images were superimposed (Overlay) to detect areas of colocalization (orange/yellow). (C, right) COS7 cells transfected with pcDNA-hPAP2a or pcDNA-hPAP2b were analyzed for PAP2b by Western blotting (10 μg/lane).

C COS 7 cells

Subcellular Localization of Endogenous and Overexpressed PAP2b

The distribution of endogenous PAP2b was examined by indirect immunofluorescence staining in Swiss 3T3 cells using our affinity-purified anti-PAP2b primary antibody and rhodamine-conjugated secondary antibody. Analysis of the fluorescence-staining pattern by confocal microscopy revealed staining in concentrated areas near the cell border (Figure 4A, arrows) and in the perinuclear region, most likely representing the Golgi because a similar staining pattern was observed when Swiss 3T3 cells were labeled with NBD-ceramide (our unpublished results). Significant stain-

ing was not observed when the anti-peptide PAP2b antibody was preincubated with the peptide (Figure 4A). Localization of PAP2b was also examined biochemically. Cytosolic, TX100-soluble, and TX100-insoluble fractions (equal cell equivalents) were prepared from Swiss 3T3 cells as described in MATERIALS AND METHODS. As shown in Figure 4A (right), PAP2b localized to the particulate fractions, and a considerable amount (~40%) was also found in the detergent-insoluble fraction. PAP2b was not detected in the cytosolic fraction.

We also examined the subcellular location of transiently expressed human PAP2b in HEK 293 cells (Figure 4B) or in COS7 cells (Figure 4C). Confocal fluorescence microscopy revealed that in HEK 293 cells, PAP2b localized to the cell periphery, suggesting plasma membrane localization (Figure 4B, arrows). Western blot analysis demonstrated that PAP2b was expressed as two immunoreactive species (Figure 4B, left) in transiently transfected HEK 293 cells of mobilities similar to those observed for the endogenous protein expressed in Swiss 3T3 cells (Figure 4A, left). In contrast, when PAP2b was expressed in COS7 cells, staining predominantly overlapped the pattern seen with an ER marker, BiP (Figure 4C). Significant staining was not observed in cells transfected with either vector alone (our unpublished results) or with pcDNA–hPAP2a (Figure 4C). Western blot analysis revealed that the majority of PAP2b was expressed as the faster-migrating form in COS7 cells (Figure 4C, right). These data and observations by Barila *et al.* (1996) and Kai *et al.* (1997) suggest that the localization and posttranslational modification of PAP2b is cell specific.

PAP 2b Is Present in Caveolin-enriched Detergent-resistant Membrane Domains

Previous reports have used β-DOG to effectively extract PAP2 from cellular membranes (Kanoh *et al.*, 1992; Kai *et al.*, 1996). β-DOG is often used to aid in the solubilization of membrane proteins that are resistant to extraction with TX100. These proteins often associate with DRMs, a type of specialized compartment enriched in cholesterol and sphingolipids (Brown and London, 1998). These studies, and the observation that PAP2b is partially insoluble in TX100, prompted us to investigate a possible association of PAP2b with DRMs. DRMs, also referred to as "cholesterol and sphingolipids rafts" (Simons and Ikonen, 1997), can be isolated from bulk plasma membranes and cytoskeletal elements by virtue of a combination of their insolubility at 4°C in nonionic detergents such as TX100 and their floatation (low density) in a sucrose density gradient (Brown and Rose, 1992).

Sucrose density gradients of TX100 extracts of Swiss 3T3 cells were prepared using the method of Brown and Rose (1992) as described in MATERIALS AND METHODS. Western blotting of the gradient fractions showed that PAP2b is present in the DRM fractions (fractions 1–3) as well as the later TX100 soluble fractions (fractions 9–12) prepared from Swiss 3T3 cells TX100 lysates (Figure 5A). Most of the cellular proteins were localized toward the bottom of the gradient (fractions 9–12) as measured by Ponceau S staining of the nitrocellulose blot (our unpublished results). These data demonstrate that PAP2b is present in DRMs prepared from Swiss 3T3 cells. Approximately 10–15% of the total PAP2 activity was associated with the DRM fraction (Figure 5A),

and this activity was resistant to *N*-ethylmaleimide (our unpublished results). PAP activity was also verified by measuring the conversion of NBD-PA to NBD-DG (our unpublished results).

Plasma membrane invaginations called caveolae, which contain a structural protein called caveolin, have similar physical properties as DRMs and as such DRMs may contain caveolin when isolated by density fractionation of detergent extracts (Kurzchalia *et al.*, 1992; Rothberg *et al.*, 1992). As shown in Figure 5, the DRM fractions prepared from Swiss 3T3 cells (Figure 5A) or HEK 293 cells (Figure 5B) were enriched in caveolin. In addition, the DRM fraction (1–3) excluded plasma membrane and intracellular membrane proteins such as the transferrin receptor (TfR), adaptin 2 (AP2), calnexin (caln), and the small G protein Rab5, which were present in the TX100-soluble fractions (Figure 5, A and B, fractions 9–12). These data suggest that fractions 1–3 are highly enriched with DRMs. HEK 293 cells also express PAP2b, albeit at much lower levels than Swiss 3T3 cells (our unpublished results). When sufficient HEK 293 cell material was fractionated ($>5 \times 10^7$ cells per gradient) (Figure 5B), immunoreactive PAP2b behaved similarly to the protein extracted for Swiss 3T3 cells (~5×10^6 cells per gradient) (Figure 5A).

Saponin sequesters cholesterol and thereby destabilizes DRM structure, rendering them sensitive to solubilization by nonionic detergents (Cerneus *et al.*, 1993; Schroeder *et al.*, 1998). Inclusion of saponin resulted in the solubilization of PAP2b and most of the caveolin present in the DRM fractions (Figure 5C). Taken together, these results indicate that DRMs prepared from Swiss 3T3 cells have properties very similar to DRMs prepared from other cell types (Montixi *et al.*, 1998). To determine the selectivity of association of PAP2b and DRMs, TX100 lysates from HEK 293 cells expressing PAP2a or PAP2b were fractionated on sucrose density gradients and assayed for PAP2 activity. PAP2 activity from HEK 293 cells expressing PAP2b (~15% of the total) and not from HEK 293 cells expressing PAP2a was detected in the DRM fractions (Figure 5D). These data suggest that PAP2b is selectively localized in DRMs.

Detergent-resistant Membrane Microdomains Contain an Active PLD/PAP Pathway

Two mammalian PLDs have been cloned and expressed (Hammond *et al.*, 1995; Colley *et al.*, 1997). Both isozymes are specific for PC and are activated by PI(4,5)P$_2$ in vitro. PLD1 is activated in vitro by ADP-ribosylation factor (Arf), by Rho family GTP-binding proteins, and by the conventional PKCs in vitro. In contrast, these same proteins do not affect the catalytic activity of PLD2 (Colley *et al.*, 1997). To characterize the PLD activity in Swiss 3T3 cells, membranes were prepared and analyzed for PLD activity in the presence of 1-butanol (Figure 6A). Membranes from Swiss 3T3 cells contained a PLD activity that was not significantly changed by the addition of GTPγS-activated Arf-1, GTPγS-activated RhoA, or PKCα (Figure 6A). To exclude the possibility that other activators were present in the cytosol, membranes were assayed in the presence of cytosol with or without GTPγS (Figure 6A). In all cases, PLD activity in Swiss 3T3 cell membranes measured in vitro behaved like the characterized in vitro activity of the recombinant PLD2 enzyme.
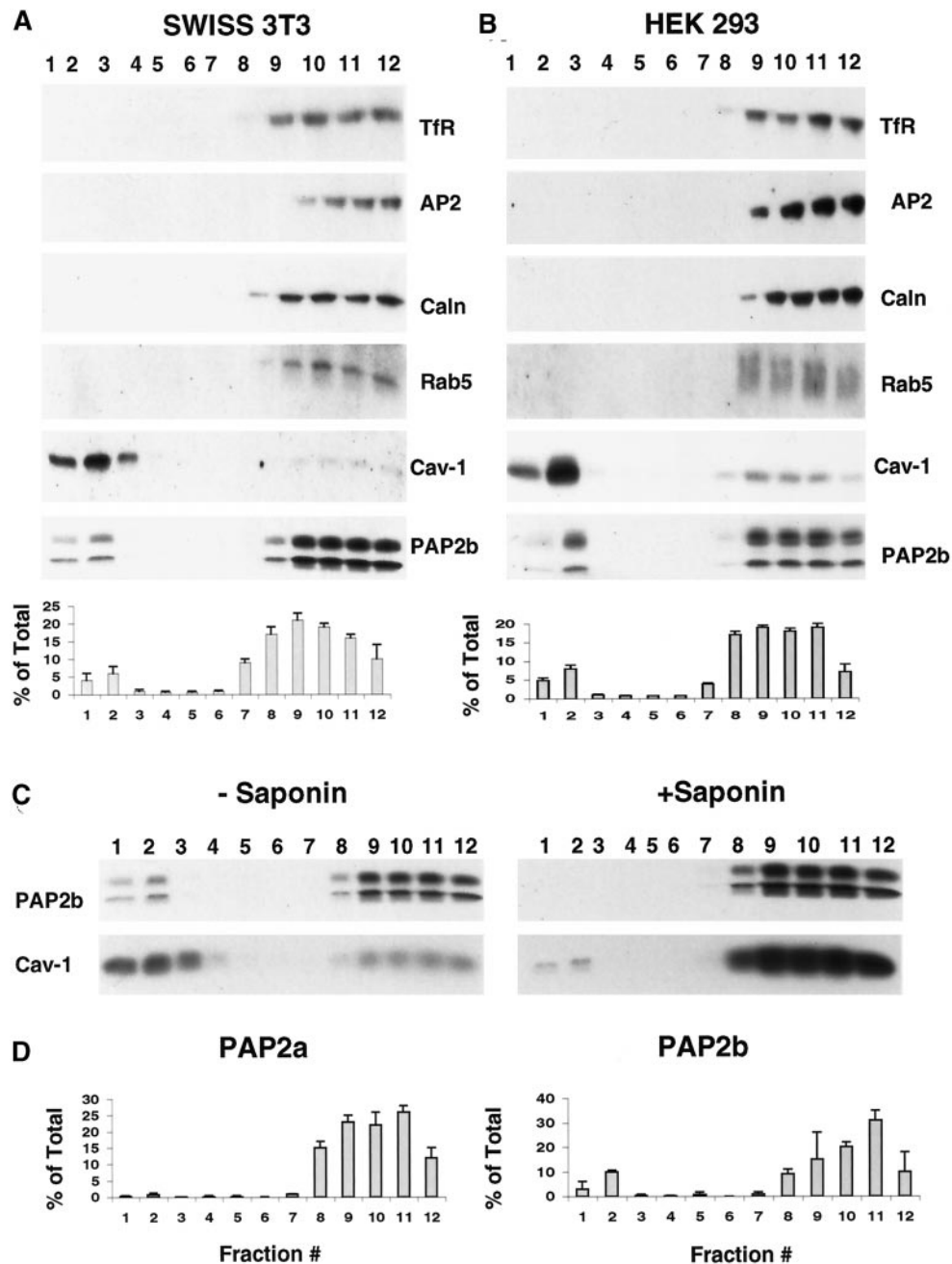
Figure 5. PAP2b localizes to caveolin-enriched detergent-resistant membrane domains. Swiss 3T3 cells (A) or HEK 293 cells (B) were lysed in 1% TX100 at 4°C and fractionated on a sucrose density gradient (two 100-mm dishes of confluent cells per gradient) as described in MATERIALS AND METHODS. Aliquots (1 ml) were collected with fraction 1 representing the top of the gradient and fraction 12 representing the bottom. Protein distribution in one-thirtieth of each fraction was analyzed for indicated proteins (TfR, transferrin receptor; AP2, adaptin; caln, calnexin; cav-1, caveolin) by Western blotting with the corresponding specific antibody as described in MATERIALS AND METHODS. Thirty microliters of each fraction (1 ml total) were assayed for PAP activity using 100 μM PA/1 mM TX100 as substrate for 30 min at 37°C and expressed as a percentage of activity in each fraction of the total (mean ± SD of triplicate determinations.) Note: there is two to three times more protein in the HEK 293 cell lysate as compared with the Swiss 3T3 cell lysate. (C) Swiss 3T3 cells were lysed in 1% TX100 in the presence (+) or absence (−) of 0.2% saponin at 4°C and fractionated as described above. One-thirtieth of each fraction was analyzed for the distribution of Cav-1 and PAP2b by Western blotting. (D) HEK 293 cells were transfected with pcDNA (vector), pcDNA-hPAP2a, or pcDNA-hPAP2b as described in MATERIALS AND METHODS, lysed in 1% TX100 at 4°C, and fractionated on a sucrose density gradient (six 10-mm dishes per gradient). Thirty microliters of each fraction (1 ml total) was assayed for PAP activity as described above. PAP activity in each fraction was corrected by subtracting activity from vector-transfected cells and expressed as a percentage of activity in each fraction of the total (mean ± SD of triplicate determinations.). Similar results were obtained in two independent experiments.
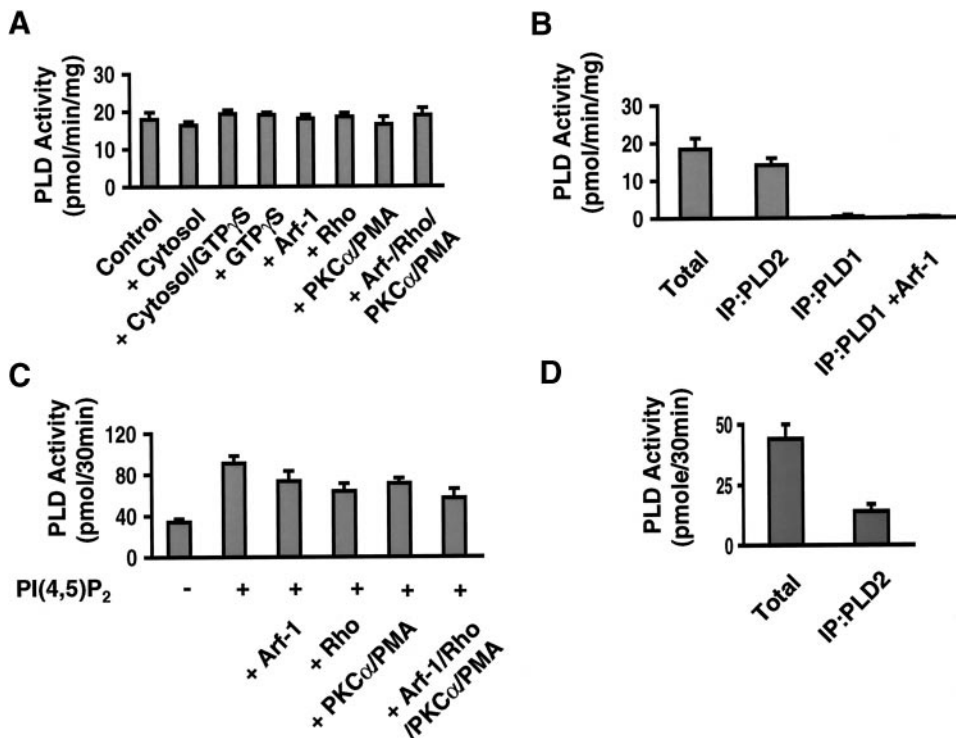
Figure 6. PLD2 is present in detergent-resistant membrane microdomains. (A) Membranes (50 μg) were prepared from Swiss 3T3 cells and analyzed for PLD activity using BODIPY-PC as substrate in the presence of 1-butanol and the indicated activators (12 μg of Swiss 3T3 cell cytosol, 100 μM GTPγS, 1 μM Arf-1, 1 μM Rho, or 70 nM PKCα and 100 nM PMA). (B) PLD (1 or 2) was immunoprecipitated from Swiss 3T3 membranes (150 μg per IP). Immune complexes were resuspended in PBS and assayed for PLD activity using BODIPY-PC as substrate. (C) DRMs (from 12 100-mm dishes) were prepared and assayed for PLD activity in the presence or absence of 5 μM PI(4,5)P$_2$ and the indicated activators (3 μM Arf-1, 2 μM Rho, or 70 nM PKCα and 100 nM PMA). (D) PLD2 was immunoprecipitated from DRM fraction as described in MATERIALS AND METHODS and assayed for PLD activity as described in B. Activity is expressed as picomoles of BODIPY-PC converted to BODIPY-PdtBuOH (or BODIPY-PA) per 30 min (the mean $\pm$ SD, n = 3). Similar results were obtained in two independent experiments.

To provide additional evidence of the identity of the PLD in Swiss 3T3 cells, we used antibodies to PLD1 (Hammond *et al.*, 1997) or PLD2 (Colley *et al.*, 1997) for immunoprecipitation analysis. The selectivity of the isozyme-specific antibodies was first investigated by immunoprecipitating PLD from baculovirus-infected Sf9 cells expressing human PLD1 or mouse PLD2. As shown in Table 2, the PLD antibodies immunoprecipitated PLD activity only in the corresponding Sf9 cell lysate. Moreover, both antibodies were efficient in immunoprecipitating their respective proteins from whole-cell lysates: antibodies against PLD1 immunoprecipitated 95% of the total activity, whereas antibodies against PLD2 immunoprecipitated 88% of the total activity. Although this antibody was made against human PLD1, it should recognize PLD1 expressed in Swiss 3T3 cells (a mouse-derived cell line) because the antibody was made using a peptide corresponding to residues 1–15 of the sequence to human PLD1 (Hammond *et al.*, 1997), which is very similar (all but three residues are identical) to mouse PLD1 (Colley *et al.*, 1997). In addition, an Arf-1–responsive PLD activity could be immunoprecipitated using this antibody from detergent extracts prepared from mouse kidney and brain (our unpublished results). At this time, the mouse PLD1 cDNA has not been ectopically expressed, and we therefore cannot determine the efficiency of immunoprecipitation.

PLD1 and PLD2 were immunoprecipitated using PLD1 and PLD2 isoform-specific antibodies from total membranes prepared from Swiss 3T3 cells and assayed for PLD activity (Figure 6B). We did not detect PLD activity in PLD1 immunoprecipitates when assayed in the presence of Arf-1. To verify the ability of Arf-1 to activate immunoprecipitated PLD1, PLD1 was immunoprecipitated from HL60 cells re-

sulting in a fivefold increase in PLD activity in the presence of Arf-1 (our unpublished results and Rudge *et al.* [1998a[). In contrast, PLD2-type activity can be immunoprecipitated from Swiss 3T3 cells using the antibody to PLD2 (Figure 6B). The activity immunoprecipitated using the PLD2 antibody recovered ~80% of the total PLD activity in Swiss 3T3 cell membranes (Figure 6B). These results suggest that Swiss 3T3 cells express PLD2 as their major PLD. Although the antibodies used in this report are effective in immunoprecipitating activity characteristic of in vitro properties reported previously (Hammond *et al.*, 1995; Colley *et al.*, 1997), unfortunately, we have not conclusively identified the corre-

**Table 2.** Specificity and efficiency of PLD antibodies

	PLD activity (pmol/30 min)[a]	
	PLD1-expressing Sf9 cells[b]	PLD2-expressing Sf9 cells
Total in lysate	17.8 $\pm$ 0.1	195 $\pm$ 7
IP/PLD1	16.9 $\pm$ 0.2 (95%)	0.9 $\pm$ 0.1
IP/PLD2	0.09 $\pm$ 0.003	172 $\pm$ 5 (88%)

Parentheses indicate the percentage activity immunoprecipitated of the total activity.

[a] PLD activity was measured using L-dipalmitoyl phosphatidyl [methyl-^{3}H] choline following the method of Brown *et al.* (1993). Activity is expressed as the means $\pm$ SD of triplicate determinations.
[b] PLD1 assayed in the presence of 6 μM Arf preactivated with GTPγS.

Figure 7. Formation of DG by PLD/PAP pathway in caveolin-enriched DRMs in vivo. (A) PLD2 was immunoprecipitated from one 100-mm dish of confluent fibroblasts per IP. DRMs and immune complexes were resuspended in 30 μl of PBS and assayed in the presence or absence of 5 μM PI(4,5)P$_2$ using NBD-PC as substrate. Lipids were extracted and separated by TLC (chloroform/methanol/acetic acid, 65:15:3, vol/vol). NBD-labeled lipids were viewed using a UV-transilluminator (UVP, Upland, CA). A negative image of the TLC plate is shown. (B) DRMs were prepared from two 100-mm dishes of Swiss 3T3 cells that were treated with or without 100 nM PMA for 30 min in the presence or absence of 1-butanol. Lipids were extracted and DG levels were determined using DG kinase and ^{32}P-γ-ATP as described in MATERIALS AND METHODS. Data are expressed as the fold increase of DG over unstimulated cells (Control). DG levels after PMA treatment are the mean $\pm$ SD of five independent experiments, and DG levels in PMA treated in the presence of butanol are the mean $\pm$ SD of three independent experiments.
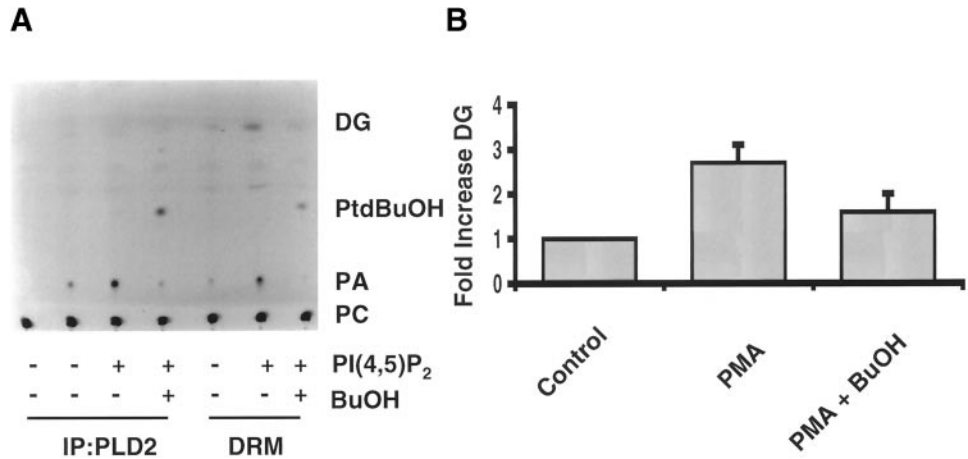
sponding endogenous proteins by Western analysis. Likewise, it is also possible that Swiss 3T3 cells contain both PLD1 and PLD2; however, PLD1 activity may not be detected because of the sensitivity of the assay used.

The distribution of PLD activity in sucrose density gradient fractions of Swiss 3T3 cell TX100 lysates was determined using [^{32}P]-PC and 1-butanol. Approximately 50% of the total PLD activity was present in DRM fractions assayed in vitro with only PI(4,5)P$_2$ as the sole exogenously added activator (our unpublished results). Because PLD activity is sensitive to the presence of detergents, DRMs were harvested from the gradients (2 ml from top) and washed extensively in cold PBS as described in MATERIALS AND METHODS. PLD activity was determined in DRMs in the presence of the indicated activators shown in Figure 6C. Substantial activity could be detected without the inclusion of PI(4,5)P$_2$; however, only PI(4,5)P$_2$ caused activation in vitro (two- to threefold) (Figure 6C). Hodgkin et al. (1999) recently reported a PLD activity in the detergent-insoluble fraction of HL60 cells that required the combined addition of Arf-1, RhoA, and PKCα for optimal in vitro activity. Although the combination of these factors caused activation of purified recombinant human PLD1 (Hammond et al. [1997] and our unpublished results), they did not enhance the PLD activity present in DRM fractions prepared from Swiss 3T3 cells (Figure 6C). These data suggest that PLD2-like activity is responsible for the PLD activity associated with DRMs. Consistent with these observations, PLD activity in DRMs can be immunoprecipitated using the PLD2 antibody (Figure 6D), and no activity was detected when this material was immunoprecipitated using the PLD1 antibody assayed in the presence of Arf-1 (our unpublished results).

When measuring PLD activity in DRMs using fluorescently labeled PC, we consistently observed the formation of DG when PI(4,5)P$_2$ was included in the substrate vesicles (Figure 7A). These results suggest that a PAP activity can act sequentially with PLD to generate DG. The inclusion of 1-butanol in the assay attenuated the DG formation (Figure 7A), whereas 2-butanol was without effect (our unpublished results). Moreover, PAP2 activity in DRMs can be immunoprecipitated using the PAP2b antibody (our unpublished results). PMA, bombesin, and sphingosine-1-phosphate can stimulate an endogenous PLD activity in Swiss 3T3 cells (Cook and Wakelam, 1992; Desai et al., 1992). To determine whether the PLD/PAP pathway could generate DG in DRMs in intact cells, DG levels in DRMs were measured from unstimulated cells or from cells that had been stimulated with PMA in the presence or absence of 1-butanol by using DG kinase and [^{32}P]-γ-ATP (Cook and Wakelam, 1992). PMA stimulated DG formation in DRMs (approximately threefold), and this increase was attenuated when cells were stimulated in the presence of 1-butanol (Figure 7). These results indicate that DG formation is dependent on PLD. Furthermore, our results suggest that PAP2b acts sequentially with PLD2 to increase a pool of DG in DRMs in intact cells.

DISCUSSION

The results presented in this study provide evidence that PAP2b can dephosphorylate PA derived from PLD generating DG. HEK 293 cells expressing PAP2b accumulated significantly more DG than control cells when stimulated with PMA (Table 1). Because the expression of PAP2b did not influence the activity of endogenous PLD in HEK 293 cells, this result suggests that PAP2b has access to PA generated by PLD. Our studies suggest that this may be accomplished by localization to specific regions of the cell where PC hydrolysis by PLD is taking place.

Immunofluorescence studies using a novel, isoform-specific antibody revealed that endogenous PAP2b localized to the cell periphery and perinuclear region (most likely Golgi) in Swiss 3T3 cells. Because PAP2b is a glycoprotein that traffics through the Golgi (Figure 3), it is not unexpected that it localizes to both the cell periphery and Golgi (Figure 4A).

This is in contrast to Dri42, the rat homologue of human PAP2b (94% identity), which has been reported to localize solely in the ER in rat intestinal epithelial cells (Barila *et al.* 1996). Although when expressed in HEK 293 cells PAP2b localized to the plasma membrane, when expressed in COS7 cells PAP2b was modified and localized similarly to Dri42 (Figure 4C). It is possible that overexpression of PAP2b/ Dri42 in COS7 or intestinal epithelial cells results in mislocalized or improperly modified proteins. A more interesting possibility is that the localization and glycosylation of PAP2b is cell type specific. This heterogeneity is most evident in that glycosylated and nonglycosylated species of PAP2b were found differentially expressed in select mouse tissues (Figure 2A).

Cellular signaling systems exhibit a high degree of specificity and efficiency that can be achieved by compartmentalization through protein–protein or protein–lipid interactions (Pawson and Scott, 1997). Unlike soluble intracellular signals, lipid signals such as PA are confined to the membrane compartments in which they are formed. Specific localization of endogenous PLD isoforms has been hampered because of the lack of suitable antibody reagents and has therefore relied on detection of catalytic activities in vitro or examination of overexpressed, epitope-tagged proteins by immunofluorescence microscopy. Nevertheless, PLD (either 1 or 2) has been localized to various cellular compartments, including the plasma membrane and secretory granules (Colley *et al.*, 1997; Morgan *et al.*, 1997; Brown *et al.*, 1998), lysosomes (Brown *et al.*, 1998; Arneson *et al.*, 1999; Toda *et al.*, 1999), Golgi and ER (Ktistakis *et al.*, 1996; Colley *et al.*, 1997), and the cytoskeleton (Hodgkin *et al.*, 1999; Iyer and Kusner, 1999).

Consistent with observations in this study (Figure 6), Czarny *et al.* (1999) concluded that PLD2 and not PLD1 is enriched in low-density TX100-insoluble membrane domains prepared from many different cell types. Here, we provide additional evidence that both PLD2 and PAP2b localize and function sequentially in DRMs, a specialized membrane compartment implicated in cellular signaling (Simons and Ikonen, 1997; Brown and London, 1998). The unique lipid and protein composition of DRMs may provide a more favorable environment for PLD2 activation, or unidentified activators may be recruited to these specialized domains on cellular activation. Besides $PI(4,5)P_2$, no other activators of PLD2 have thus far been identified. As reported for inositol lipid-specific phospholipase C (Glaser *et al.*, 1996), sequestration of $PI(4,5)P_2$ within membrane domains may control PLD activity, and it has been demonstrated that $PI(4,5)P_2$ is selectively enriched in DRMs (Hope and Pike, 1996).

There are at least four mammalian PAP2 isoenzymes, and it is presently unclear whether these have redundant, overlapping, or distinct functions. Although mRNA for PAP2b was found in most human tissues (Kai *et al.*, 1997), we found that levels of PAP2b protein varied substantially between tissues, suggesting that this PAP2 isoform may have a cell- or tissue-specific function. Our results suggest that one function of PAP2b is to dephosphorylate PA generated by PLD. Unlike PAP2b, expression of PAP2a in HEK 293 cells did not significantly alter DG levels when cells were stimulated with PMA. It has been suggested that PAP2a acts partly as an ectoenzyme capable of degrading exogenous lipid mono-

phosphates (Roberts, *et al.* 1998; Jasinska *et al.*, 1999) and thereby attenuating specific extracellular lipid signals (Jasinska *et al.*, 1999). PAP2a and PAP2b share the same putative transmembrane topology (Barila *et al.*, 1996), which would place the active site of the enzymes in the lumenal or extracellular space. The mechanisms by which PAP2b gains access to PA generated intracellularly are unclear. Yeast PAP2 homologues clearly play roles in the metabolism of intracellular PA because deletion of these genes results in significant increases in intracellular levels of PA (Toke *et al.*, 1998).

Because PA is a potent lipid mediator, PAP may terminate the PA signal by converting it to DG. It is not yet clear whether the DG generated in this manner is competent as an intracellular signal (Wakelam, 1998). Liu and Anderson (1995) reported that DG is present in caveolin-enriched membrane domains isolated from human fibroblasts and that hormonal stimulation resulted in a significant increase in DG in this fraction. The source of DG in these experiments was not defined. Our results indicate that the PLD/PAP pathway is active in DRMs and generates DG. Because DG has been identified as a physiological activator of PKC (Nishizuka, 1995), it has been postulated that the PLD/PAP pathway plays a major role in the formation of DG from PC to prolong PKC activation or to sensitize PKC for stimulation by subsequent increases in intracellular calcium (Exton, 1997). To date, however, there is no clear evidence to support a functional role for DG generated by the PLD/PAP pathway in the activation of PKC in vivo (Wakelam, 1998). Alternatively, other DG-binding proteins have been identified (Topham and Prescott, 1999) and perhaps are regulated by the PLD/PAP pathway. In addition to its second messenger role, DG can be metabolized to triglycerides or glycerophospholipids. Deletions of genes encoding PAP2-like enzymes in yeast (LPP1 and DPP1) resulted in decreases in phosphatidylinositol levels (Toke *et al.*, 1998), suggesting a putative role of PAP2 in glycerophospholipid synthesis. PAP2 enzymes may therefore play a central role both in DG formation in agonist-stimulated cells and in control of glycerophospholipid biosynthesis.

In summary, our results demonstrate that at least one isoform of the type 2 PAPs, PAP2b, can dephosphorylate PLD-derived PA in vivo. Our results indicate that the PLD/ PAP pathway is active in caveolin-enriched DRMs where the lipid composition and physical factors operating in these membranes may provide a selective environment for the regulation and actions of enzymes involved in signaling through PC hydrolysis. Further characterization of these lipid-modifying enzymes should aid in defining the physiological roles of PA and DG as second messengers generated from the PLD/PAP pathway.

ACKNOWLEDGMENTS

REFERENCES

Arneson, L.S., Kunz, J., Anderson, R.A., and Traub, L.M. (1999). Coupled inositide phosphorylation and phospholipase D activation initiates clathrin-coat assembly on lysosomes. J. Biol. Chem. *274*, 17794–17805.

Barila, D., Plateroti, M., Nobili, F., Onetti Muda, A., Xie, Y., Morimoto, T., and Perozzi, G. (1996). The Dri 42 gene, whose expression is up-regulated during epithelial differentiation, encodes a novel endoplasmic reticulum resident transmembrane protein. J. Biol. Chem. *271*, 29928–29936.

Berridge, M.J. (1993). Inositol trisphosphate and calcium signaling. Nature *361*, 315–325.

Bligh E.J., and Dyer, W.J. (1959). A rapid method of total lipid extraction and purification. Can. J. Biochem. Pharmacol. *37*, 911–917.

Bradford, M.M. (1976). A rapid and sensitive method for the quantitation of microgram quantities of protein utilizing the principle of protein-dye binding. Anal. Biochem. *72*, 248–254.

Brindley, D.N., and Waggoner, D.W. (1996). Phosphatidate phosphohydrolase and signal transduction. Chem. Phys. Lipids *80*, 45–57.

Brindley, D,N., and Waggoner, D.W. (1998). Mammalian lipid phosphate phosphohydrolases. J. Biol. Chem. *273*, 24281–24284.

Brown, D.A., and London, E. (1998). Functions of lipid rafts in biological membranes. Annu. Rev. Cell Dev. Biol. *14*, 111–136.

Brown, D.A., and Rose, J.K. (1992). Sorting of GPI-anchored proteins to glycolipid-enriched membranes subdomains during transport to the apical cell surface. Cell *68*, 533–544.

Brown, F.D., Thompson, N., Saqib, K.M., Clark, J.M., Powner, D., Thompson, N.T., Solari, R., and Wakelam, M.J. (1998). Phospholipase D1 localizes to secretory granules and lysosomes and is plasma-membrane translocated on cellular stimulation. Curr. Biol. *8*, 835–838.

Brown, H.A., Gutowski, S., Moomaw, C.R., Slaughter, C., and Sternweis, P.C. (1993). ADP-ribosylation factor, a small GTP-dependent regulatory protein, stimulates phospholipase D activity. Cell *75*, 1137–1144.

Cerneus, D.P., Ueffing, E., Posthuma, G., Strous, G. J., and van der Ende, A. (1993) Detergent insolubility of alkaline phosphatase during biosynthetic transport and endocytosis. Role of cholesterol. J. Biol. Chem. *268*, 3150–3155.

Colley, W.C., Sung, T-C., Roll, R., Jenco, J., Hammond, S.M., Altshuller, Y., Bar-Sagi, D., Morris, A.J., and Frohman, M.A. (1997). Phospholipase D2, a distinct phospholipase D isoform with novel regulatory properties that provokes cytoskeletal reorganization. Curr. Biol. *7*, 191–201.

Cook, S.J., and Wakelam, M.J.O. (1992). EGF increases sn-1,2 diglyceride levels and activates PLD-catalyzed PC breakdown in Swiss 3T3 cells in the absence of inositol lipid hydrolysis. Biochem. J. *285*, 247–253.

Czarny, M., Lavie, Y., Fiucci, G., and Liscovitch, M. (1999). Localization of phospholipase D in detergent-insoluble, caveolin-rich membrane domains. J. Biol. Chem. *274*, 2717–2724.

Desai, N.N. Zhang, H., Olivera, A., Mattie, M.E., and Spiegel, S. (1992). Sphingosine-1-phosphate, a metabolite of sphingosine, increases phosphatidic acid levels by phospholipase D activation. J. Biol. Chem. *267*, 23122–23128.

Divecha N., and Irvine R.F. (1995). Phospholipid signaling. Cell *80*, 269–278.

Exton, J.H. (1997). New developments in phospholipase D. J. Biol. Chem. *272*, 15579–15582.

Ghosh, S., Strum, J.C., Sciorra, V.A., Daniel, L.W., and Bell, R.M. (1996). Raf-1 kinase possesses distinct binding domains for PS and PA: PA regulates the translocation of Raf-1 in TPA-stimulated MDCK cells. J. Biol. Chem. *271*, 8472–8480.

Glaser, M., Wanaski, S., Buser, C.A., Boguslavsky, V., Rashidzada, W., Morris, A., Rebecchi, M., Scarlata, S.F., Runnels, L.W., Prestwich, G.D., Chen, J., Aderem, A., Ahn, J., and McLaughlin, S. (1996). MARKs produces reversible inhibition of phospholipase C by sequestering phosphatidylinositol 4,5,bisphosphate in lateral domains. J. Biol. Chem. *271*, 26187–26193.

Hammond, S.M., Altshuller Y.M., Sung, T.-C., Rudge S.A., Rose, K.A., Engebrecht, J., Morris A.J., and Frohman, M.A. (1995). Human ADP-ribosylation factor-activated phosphatidylcholine-specific phospholipase D defines a new and highly conserved gene family. J. Biol. Chem. *270*, 29640–29643.

Hammond, S.M., Jenco, J.M., Nakashima, S., Cadwallader, K., Gu, Q., Cook, S., Nozawa, Y., Prestwich, G.D., Frohman, M.A., and Morris, A.J. (1997). Characterization of two alternately spliced forms of phospholipase D1. Activation of the purified enzymes by phosphatidylinositol 4,5-bisphosphate, ADP-ribosylation factor, and Rho family monomeric GTP-binding proteins and protein kinase C-alpha. J. Biol. Chem. *272*, 3860–3868.

Harlow, E., and Lane, D. (1988). Antibodies: A Laboratory Manual, Cold Spring Harbor, NY: Cold Spring Harbor Laboratory.

Hodgkin, M.N., Clark, J.M., Rose, S., Saqib, K., and Wakelam, M.J. (1999). Characterization of the regulation of phospholipase D activity in the detergent-insoluble fraction of HL60 cells by protein kinase C and small G-proteins. Biochem. J. *339*, 87–93.

Hooks, S.B., Ragan S.P., and Lynch, K.R. (1998). Identification of a novel human phosphatidic acid phosphatase type 2 isoform. FEBS Lett *427*, 188–193.

Hope, H.R., and Pike. L.J. (1996). Phosphoinositides and phosphoinositide-utilizing enzymes in detergent-insoluble lipid domains. Mol. Biol. Cell *7*, 843–851.

Iyer, S.S., and Kusner, D.J. (1999). Association of phospholipase D activity with the detergent-insoluble cytoskeleton of U937 promonocytic leukocytes. J. Biol. Chem. *274*, 2350–2359.

Jamal, Z., Martin, A., Gomez-Munoz, A., and Brindley, D.N. (1991). Plasma membrane fractions from rat liver contain a phosphatidate phospho-hydrolase distinct from that in the endoplasmic reticulum and cytosol. J. Biol. Chem. *266*, 2988–2996.

Jasinska, R., Zhang, Q.X., Pilquil, C., Singh, I., Xu, J., Dewald, J., Dillon, D.A., Berthiaume, L.G., Carman, G.M., Waggoner, D.W., and Brindley, D.N. (1999). Lipid phosphate phosphohydrolase-1 degrades exogenous glycerolipid and sphingolipid phosphate esters. Biochem. J. *340*, 677–686.

Kai, M., Wada, I., Imai, S., Sakane, F., and Kanoh, H. (1996). Identification and cDNA cloning of 35 kDa phosphatidic acid phosphatase (type 2) bound to plasma membranes. J. Biol. Chem. *271*, 18931–18938.

Kai, M., Wada, I., Imai, S., Sakane, F., and Kanoh, H. (1997). Cloning and characterization of two human isozymes of Mg^{+2}-independent phosphatidic acid phosphatase. J. Biol. Chem. *272*, 24572–24578.

Kanoh, H., Imai, S., Yamada, K., and Sakane, F. (1992). Purification and properties of phosphatidic acid phosphatase from porcine thymus membranes. J. Biol. Chem. *267*, 25309–25314.

Ktistakis, N.T., Brown, H.A., Waters, M.G., Strenweis, P.C., and Roth, M.G. (1996). Evidence that PLD mediates ARF-dependent formation of Golgi coated vesicles. J. Cell Biol. *134*, 295–306.

Kurzchalia, T.V., Dupree, P., Parton, R.G., Kellner, R., Virta, H., Lehnert, M., and Simons, K. (1992). VIP21, a 21-kDa membrane

protein is an integral component of trans-Golgi network derived transport vesicles. J. Cell Biol. *118*, 1003–1014.

Leung, D.W., Tompkins, C.K., and White, T. (1998). Molecular cloning of two alternatively spliced forms of human phosphatidic acid phosphatase cDNAs that are differentially expressed in normal and tumor cells. DNA Cell Biol. *17*, 377–385.

Liu, P., and Anderson, R.G.W. (1995). Compartmentalized production of ceramide at the cell surface. J. Biol. Chem. *270*, 27179–27185.

Metz, S.A., and Dunlop, M. (1991). Inhibition of the metabolism of phosphatidylethanol and phosphatidic acid, and stimulation of insulin release, by propranol in intact pancreatic islets. Biochem. Pharmacol. 41:R1–R4.

Montixi, C., Langlet, C., Bernard, A.-M., Thimonier, J., Dubois, C., Wurbel, M.-A., Chauvin, J.-P., Pierres, M., and He, H.-T. (1998). Engagement of T cell receptor triggers its recruitment to low-density detergent-insoluble membrane domains. EMBO J. *17*, 5334–5348.

Morgan, C.P., Sengelov, H., Whatmore, J., Borregaard, N., and Cockcroft, S. (1997). ADP-ribosylation factor-regulated phospholipase D activity localizes to secretory vesicles and mobilizes to the plasma membrane following *N*-formylmethionyl-leucyl-phenylalanine stimulation of human neutrophils. Biochem. J. *325*, 581–585.

Morris, A.J., Rudge, S.A., Mahlum, C.E., and Jenco, J.M. (1995). Regulation of phosphoinositide-3-kinase by G protein beta gamma subunits in a rat osteosarcoma cell line. Mol. Pharmacol. *48*, 532–539.

Nishizuka, Y. (1995). Protein kinase C and lipid signaling for sustained cellular responses. FASEB J. *9*, 484–496.

Pai, J.K., Siegel, M.I., Egan, R.W., and Billah, M.M. (1988). Phospholipase D catalyzes phospholipid metabolism in chemotactic peptide-stimulated HL-60 granulocytes. J. Biol. Chem. *263*, 12472–12477.

Pawson, T., and Scott, J.D. (1997). Signaling through scaffold, anchoring and adaptor proteins. Science *278*, 2075–2080.

Rizzo, M.A., Shome, K., Vasudevan, C., Stolz, D.B., Sung, T.-C., Frohman, M.A., Watkins, S.C., and Romero, G. (1999). Phospholipase D and its product, phosphatidic acid, mediate agonist-dependent Raf-1 translocation to the plasma membrane and the activation of the mitogen-activated protein kinase pathway. J. Biol. Chem. *274*, 1131–1139.

Roberts, R., Sciorra, V.A., and Morris, A.J. (1998). Substrate specificity of the human type 2a, 2b, and 2c enzymes and cell surface activity of the 2a isoform. J. Biol. Chem. *273*, 22059–22067.

Rothberg, K., Heuser, J.E., Donzell, W.C., Ying, Y.-S., Glenney, J.R., and Anderson, R.G.W. (1992). Caveolin, a protein component of caveolae membrane coats. Cell *68*, 673–682.

Rudge, S.A., Cavenagh, M.M., Kamath, R., Sciorra, V.A., Morris, A.J., Kahn, R.A., and Engebrecht, J. (1998a). ADP-ribosylation factors do not activate yeast phospholipase Ds, but are required for sporulation. Mol. Biol. Cell *9*, 2025–2036.

Rudge, S.A., Morris, A.J., and Engebrecht, J. (1998b). Relocalization of phospholipase D activity mediates membrane formation during meiosis. J. Cell Biol. *140*, 81–90.

Rumenapp, U., Schmidt, M., Wahn, F., Tapp, E., Grannass, A., and Jakobs, K.H. (1997). Characteristics of PKC- and ARF-stimulated PLD activities in human embryonic kidney cells. Eur. J. Biochem. *248*, 407–414.

Schroeder, R.J., Ahmed, S.N., Zhu, Y., London, E., and Brown, D.A. (1998). Cholesterol and sphingolipid enhance the TX100 insolubility of glycosylphosphatidylinositol-anchored proteins by promoting the formation of detergent-insoluble ordered membrane domains. J. Biol. Chem. *273*, 1150–1157.

Simons, K., and Ikonen, E. (1997). Sphingolipid-cholesterol rafts in membrane trafficking and signaling. Nature *387*, 569–572.

Singer, W.D., Brown, H.A., and Sternweis, P.C. (1997). Regulation of eukaryotic phosphatidylinositol-specific phospholipase C and phospholipase D. Annu. Rev. Biochem. *66*, 475–509.

Smith, S.W., Weiss, S.B., and Kennedy, E.P. (1957). The enzymatic dephosphorylation of phosphatidic acid. J. Biol. Chem. *228*, 915–922.

Toda, K., Nogami, M., Murakami, K., Kanaho, Y., and Nakayama, K. (1999). Colocalization of phospholipase D1 and GTP-binding-defective mutant of ADP-ribosylation factor 6 to endosomes and lysosomes. FEBS Lett. *442*, 221–225.

Toke, D.A., Bennett, W.L., Oshiro, J., Wu, W.-I., Voelker, D.R., and Carman, G.M. (1998). Isolation and characterization of the *Saccharomyces cerevisiae* LPP1 gene encoding a Mg+2- independent phosphatidate phosphatase. J. Biol. Chem. *273*, 14331–14338.

Topham, M.K., and Prescott, S.M. (1999). Mammalian diacylglycerol kinases, a family of lipid kinases with signaling functions. J. Biol. Chem. *274*, 11447–11450.

Waggoner, D.W., Martin, A., Dewald, J., Gomez-Munoz, A., and Brindley, D.N. (1995). Purification and characterization of a novel plasma membrane phosphatidic phosphohydrolase from rat liver. J. Biol. Chem. *270*, 19422–19429.

Waggoner, D.W., Gomez-Munoz, A., Dewald, J., and Brindley, D.N. (1996). Phosphatidate phosphohydrolase catalyzes the hydrolysis of ceramide-1-phosphate, lysophosphatidate, and sphingosine-1-phosphate. J. Biol. Chem. *271*, 16506–16509.

Wakelam, M.J.O. (1998). Diacylglycerol: when is it an intracellular messenger? Biochim. Biophys. Acta *1436*, 117–126.